Revista Colombiana de Materiales N. 5 pp. 103-110

Edición Especial Artículos Cortos

CHARACTERIZATION OF ZnO NANOFILMS DEPOSITED BY CBD-AμW

Joel Díaz Reyes [2], Javier Martínez Juárez [1], David Hernández de la Luz [3]*
1: Ph. D., CIBA, Instituto Politécnico Nacional. Tepetitla, Tlaxcala, México
2: Ph. D., Benemérita Universidad Autónoma de Puebla, Puebla, México
3: Ph. D., Benemérita Universidad Autónoma de Puebla, Puebla, México

* Contacto: joel_diaz_reyes@hotmail.com

ABSTRACT

The physical properties of ZnO nanofilms are studied as a function of the urea concentration in the growth solution. ZnO is grown by Chemical Bath Deposition technique activated by microwaves (CBD-AμW). The chemical stoichiometry was determined by energy dispersive spectroscopy (EDS) measurements on the ZnO nanofilms. By X-rays scattering is obtained a polycrystalline hexagonal wurtzite type structure of grown ZnO films. By Raman spectroscopy is confirmed the wurtzite type structure of ZnO films and their Raman spectra show 4 main peaks at 444, 338, 104 and 78 cm^{-1} that correspond to the modes E_2^{high}, (E_2^{high} - E_2^{low}), E_2^{low}, which are associated to the oxygen and zinc sublattices and an unidentified band.

Keywords: *ZnO, Wide bandgap Semiconductor, Chemical bath deposition, X-Ray difraction*

RESUMEN

Las propiedades físicas de las nanopelículas de ZnO son estudiadas como una función de la concentración de urea en la solución de crecimiento. ZnO es crecido mediante la técnica de deposición de baño químico activado por microondas (CBD-A μW). La estequiometria química se determinó por mediciones de espectroscopia de dispersión de energía (EDS) de las nanopelículas de ZnO. Mediante dispersión de rayos X se obtiene nanopelículas de ZnO policristalina una estructura tipo hexagonal wurtzita. Por espectroscopia Raman es confirmada la estructura cristalina tipo wurtzita de las películas de ZnO y sus espectros Raman muestran 4 picos principales en 444, 338, 104 y 78 cm^{-1} que corresponden a los modos E_2^{high}, (E_2^{high} - E_2^{low}), E_2^{low}, que están asociados a las subredes del oxígeno y de zinc y una banda no identificada.

Palabras clave: *ZnO, Semiconductor de banda ancha, Deposición por baño quimico, Rayos X*

1 INTRODUCTION

Zinc oxide (ZnO) is an important semiconducting oxide because has a wide range of applications. ZnO can be used in piezoelectric devices or in optoelectronic applications, especially as a transparent electrode [1]. Its high electrical conductivity and optical transmittance in the visible region makes it useful for transparent conducting electrodes in flat panel displays or as optical windows in electroluminescent devices [2]. Among the various deposition techniques for ZnO thin films, DC reactive magnetron sputtering has received much attention, because of its flexibility, and because it offers good chemical composition control over extended areas.

Furthermore, the deposition technique offers the possibility to select the deposition rates in a wide range of values [3]. For more complex alloys, the stoichiometry of the films can be modified by changing the substrate temperature, the pressure and the reactive atmosphere used during the deposition process. Moreover the properties of the films depend too on the sputtering power and post annealing processes on the films [3]. In the present work we report the growth and the characterization of ZnO nanofilms deposited by Chemical Bath Deposition technique activated by microwaves (CBD-AμW) on corning glass at various ratios of urea.

2 EXPERIMENTAL DETAILS

As result of the chemical reactions in the CBD-AμW the ZnO is obtained in nanofilm form, whose thicknesses are around 800 nm. The solutions of the precursor reagents are prepared at room temperature using deionized water of 18.2 MΩ-cm of resistivity with the purpose of diminishing the residual impurity concentration in the material. The used molar ratios are the following: $Zn(NO_3)_2$-0.1 M, Urea-0.1, 0.2,..., 1.0 M. The samples are submerged in the solution and NH_4OH is added to it. Afterwards, they are undergoing microwave irradiation during 5 min at maximum power keeping the temperature constant and after irradiating them at lowest power for 40 min. Finally, they are rinsed with strong agitation and are dried with gaseous nitrogen. Structural characterization of the samples is carried out by means of X-ray diffraction (XRD) in a Bruker D8 Discover diffractometer, parallel beam geometry and monochromator of gobel mirror, CuKα radiation, 1.5406 Å, in the range of 20° <2θ <80° by step of 0.02°. The XRD data were refined using the programs POWDERX and DICVOL04 to determine the crystalline system, the parameters of unit cell and the density X (DX). On the other hand the measurements of energy dispersive spectroscopy (EDS) were carried out in an LEO 438VP system, with W.D. of 26 mm using a pressure of 20 Pa to obtain the chemical stoichiometry. Raman scattering experiments were performed at room temperature using the 6328 Å line of a He-Ne laser at normal incidence for excitation. The light was focused to a diameter of 6.0 μm at the sample using a 50x (numerical aperture 0.9) microscope objective. The nominal laser power used in these measurements was 20 mW. Scattered light was analysed using a micro-Raman system (Lambram model of Dilor), a 256x1024-pixel CCD used as detector cooled to 140 K using liquid nitrogen, and two interchangeable gratings (600 and 1800 g/mm).

3 EXPERIMENTAL RESULTS AND DISCUSSION

Figure 1 shows the diffractograms of the ZnO nanofilms that indicate that in all the nitrate and urea ratios, the synthesized material is ZnO and besides there is not changing of crystalline phase. ZnO has hexagonal polycrystalline wurtzite type structure and the variation in the solutions concentrations is not remarkably observed in the diffractograms, see Fig. 2. Besides, from the X-ray patterns were not possible to determine the influence of the urea concentration in the growing direction of the films as one can clearly observe in Fig. 2. The labelled indices show that all ZnO samples have the wurtzite crystalline structure and no evidence of urea-related secondary phases, within the detection limit of the instrument. ZnO commonly crystallizes in a hexagonal wurzite type structure in the most of the synthesizing methods, with lattice parameters of unit cell of $\boldsymbol{a}$ = 3.2495 Å and $\boldsymbol{c}$ = 5.2069 Å and with a density ρ around 5.605 g/cm^3 [4]. By refinement of X-ray experimental data one finds the unit cell parameters for all studied urea concentrations, which are illustrated in Fig. 3. For the ZnO nanofilms the parameter average values are $\boldsymbol{a}$ = 3.253 Å and $\boldsymbol{c}$ =

5.212 Å, with a tendency to increase in both parameters and a similar tendency to increase or decrease among their values starting from the molar relation 1:4 to 1:10. However, the tendency of lattice constant values in the molar relations 1:1, 1:2 and 1:3 is opposed, which can be explained if it is considered the stress when the nanofilm is deposited, this is valid for the three ratios. For the relation 1:4 the nanofilm is deposited with compressive stress and starting from the relation 1:5 again it is deposited with strain. From the refinement of X-ray experimental data the volume of the unit cell is obtained, besides of the lattice parameters. If it is considered that each unit cell of ZnO contains two zinc atoms and two oxygen atoms, then taking the atomic weight of the chemical elements can determine the density X (DX) of this material. Fig. 4 shows the results of the densities of the ZnO films that were synthesized by CBD-AμW. The Films density does not show a clear tendency as a function of the urea concentration changes in the growth solution, that is why it could be considered an average value of approximately 5.662 g/cm^3. However, if one only considers the ratios 1:1, 1:5 and 1:10 could be observed that the tendency is to decrease, as the urea concentration increases in the solution.

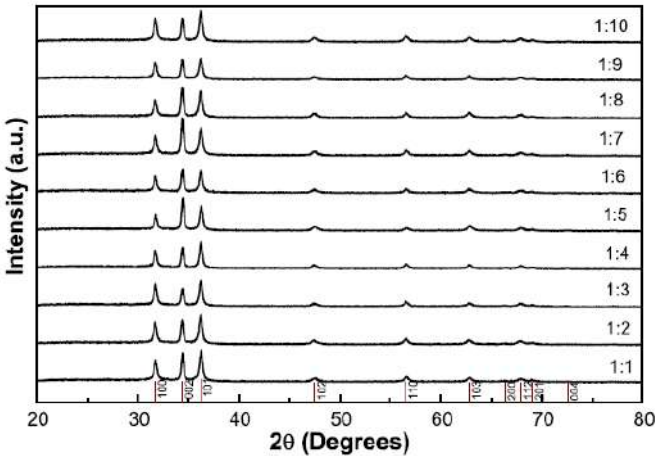

Figure 1. X-ray patterns of the ZnO nano-films synthesized by CBD-AμW.

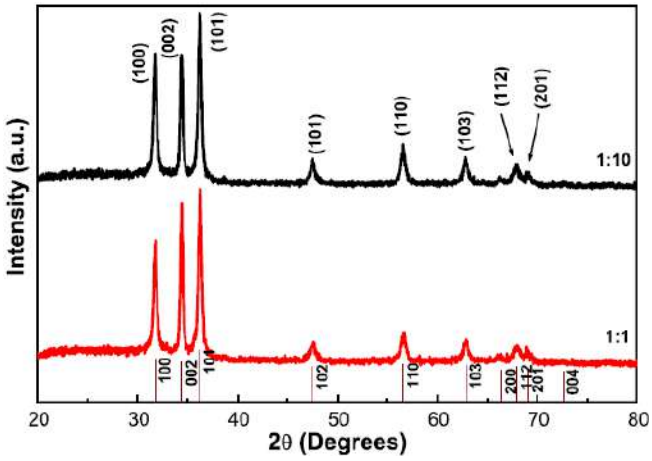

Figure 2. X-ray patterns of the ZnO nano-films with ratios 1:1 and 1:10.

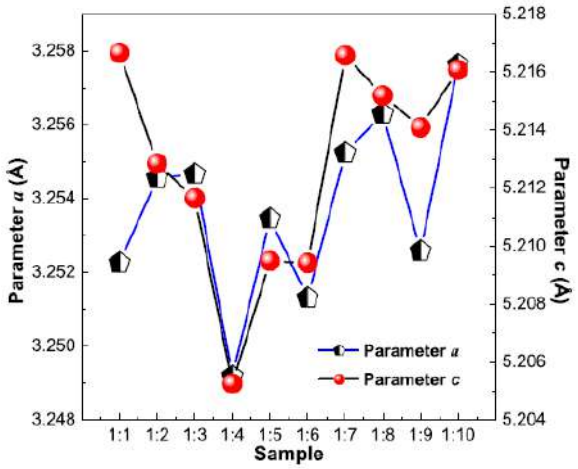

Figure 3. Lattice parameters obtained by refinement of x-ray pattern data for ZnO films.

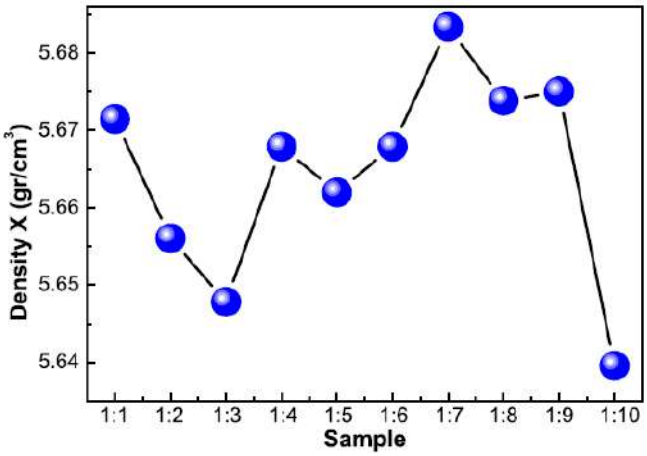

Figure 4. ZnO thin films density X for the different ratios between the zinc salt and urea.

The chemical composition of the ZnO thin films were obtained by measurements of energy dispersive spectroscopy (EDS) to the samples with ratio: 1:1, 1:5 and 1:10. The results of such measurements are shown in Table 1, in which is included the atomic and mass percentages. From these results is observed that the ratio 1:5 is the one that gives a good stoichiometric compound and that starting from it a higher urea concentration in the solution gives a greater presence of zinc in the material and an absence of oxygen. Continuing with the consideration that each unit cell contains two zinc atoms and two oxygen atoms, the atomic weight of the ideal unit cell is ~162.74 corresponding to 19.66% oxygen atoms and 80.33% zinc atoms, then when a stoichiometric deviation of ideal unit cell occurs it could establish a correspondence between vacancies or interstices of some of the compound elements (V_O, V_{Zn}, Zn_i, O_i). Assuming that the volume of the unit cell remains around 47.78 $Å^3$ for all cases and also because of the atomic weight of the zinc atom is four times greater that of oxygen atom, it could be expected that a great presence of zinc atoms in the structure should correspond to a higher density and the contrary should happen for a greater presence of oxygen atoms. However, when the EDS results are analyzed considering the densities can see that for a greater zinc concentration in the material the density diminishes, which indicates that the zinc is present interstitially in the structure in

such a way that relaxes the chemical bonds. From Table 1 is observed that the sample with ratio 1:10 contains higher zinc concentration, while the sample with ratio 1:1 contains zinc vacancies.

Table 1. Results of the analysis by EDS of the samples with the ratios 1:1, 1:5 and 1:10.

Ratio [Zinc]/[Urea]	Oxygen atomic percentage (%)	Zinc atomic percentage (%)	Oxygen mass percent (%)	Zinc mass percent (%)
1:10	47.01	52.99	17.83	82.17
1:5	50.08	49.92	19.71	80.29
1:1	52.43	47.57	21.24	78.76

Figure 5 shows polarized Raman spectra of the typical ZnO films measured in backscattering configuration, which allows the observation of all active modes. The Raman spectra show a similar behaviour and only vary in the intensity of the bands. The sample 1:4 that is closely stoichiometric presents the more intense Raman spectrum and is better resolved and as the urea concentration is increased/diminished in the solution the spectra decrease though they are nearly similar. The Raman spectra are dominated by two intense modes: sharp E_2 modes sited at 104 and 444 cm^{-1}. The low-frequency E_2 mode, involving mainly Zn motion, displays an extremely narrow line width. The E_2^{high} mode displays a clear asymmetry toward low frequencies that we shall discus in more detail below, which is associated to oxygen sublattice. The Raman spectrum can be deconvoluted in Lorentzian line shape signals through a standard fitting procedure performed in the whole studied interval and the results are plotted using solid lines, which are shown in Fig. 6. Reasonable fits are achieved with Lorentzian curves, whose frequencies are shown in figure and which allow to identify the vibrational bands present in the Raman spectrum. In contrast with previous works, where the $A_1(LO)$ mode could not be detected for excitation wavelengths longer than 406.7 nm [5], we detect a weak $A_1(LO)$ mode at 578 cm^{-1}. In addition to the strong E_2 mode a new peak appears at 388 cm^{-1}, which can be assigned to the $A_1(TO)$ mode. We detect a strong mode, a low frequency one at 104 cm^{-1}, which could be associated to the E_2^{low} mode. The $2E_2^{high}$ mode can be observed at 195 cm^{-1} in the Raman spectrum. Finally, there are two intense modes at 78 and 115 cm^{-1} that could not be identified.

One of the peaks in the intermediate-low-frequency region is observed at 338 cm^{-1}. This mode had been previously assigned to transverse acoustic overtone scattering at M [5]. However, studies made by Cuscó of temperature dependence of its Raman intensity clearly indicate that this one is a difference mode, see Fig. 5. The frequency of this mode is in good agreement with the difference between the E_2^{high} and E_2^{low} frequencies measured in our samples (340 cm^{-1}) [6]. The E_2^{high} - E_2^{low} difference contains symmetries A_1, (E_1, E_2). According to the calculated phonon dispersion relations [7], the 338 cm^{-1} mode could also contain contributions from $[TO-TA]_{A,L,H}$ differences. Another prominent peak is observed at 195 cm^{-1}, which exhibits A_1 symmetry and thus can be attributed to a TO overtone [6]. The peak at 534 cm^{-1} is of A_1 symmetry and can be attributed to $2B_1^{low}$ and LA overtones along L-M and H.

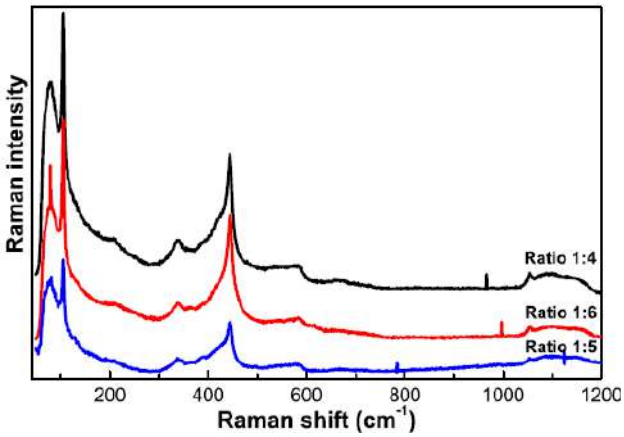

Figure 5. Raman spectra of ZnO nanofilms for molar ratios 1:4, 1:5 and 1:6.

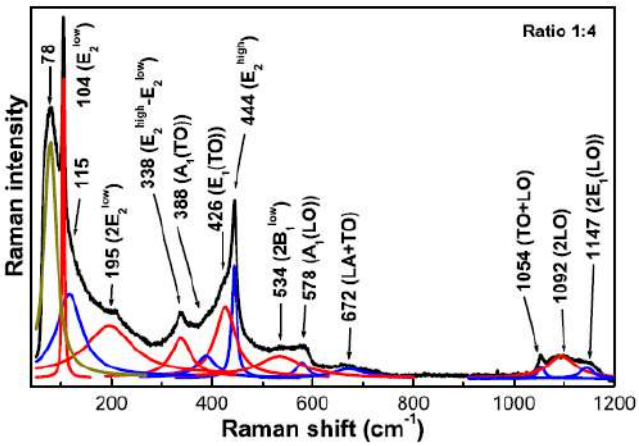

Figure 6. Curve fitting analysis of the Raman spectrum of ZnO thin film with ratio 1:4.

It is noted that the E_2^{high} mode exhibits a visibly asymmetric line shape with a low-frequency tail. This is quite apparent from Fig. 5 when one compares the line shapes of the E_2^{high} and $A_1(TO)$ modes. The asymmetry of the E_2^{high} mode cannot be ascribed to lattice disorder. Furthermore, isotopic broadening is negligible for the E_2^{high} mode since it mainly involves O motion, and O is nearly isotropically pure. The line-shape broadening is then mostly determined by anharmonic phonon-phonon interactions. These can result in strongly distorted peaks when resonant interaction with a band of second-order combinations takes place (Fermi resonance), as is the case, for instance, for the GaP TO mode [8], where the presence of van Hove-type singularities in the DOS of the *TA+LA* combination band gives rise to a highly asymmetric TO mode, which develops a side band at high pressure. A similar situation occurs for the E_2^{high} mode of ZnO, as its frequency lies close to a ridge-like structure of the two-phonon DOS corresponding to *TA+LA* combinations in the vicinity of the *K* point [9].

Whereas wavevector conservation restricts the phonons involved in first-order Raman scattering to those with **k**~0, phonons from the entire Brillouin zone take part in second order Raman scattering. Therefore, second-order spectra usually display feature-rich structures, which are determined, on the one hand, by the phonon density of states (DOS) and, on the other hand, by the selection rules of the two-phonon scattering processes. According to density-functional theory

(DFT) calculations [7] the phonon DOS of ZnO presents a frequency gap between acoustic and optical modes that extends from 270 to 410 cm^{-1}. The second-order spectra may then be divided into three regions: (i) the low-frequency region (approximately 160–540 cm^{-1}) dominated by acoustic overtones, (ii) the high-frequency region (820–1120 cm^{-1}) formed by optical overtones and combinations, and (iii) the intermediate-frequency region (540–820 cm^{-1}) where optical and acoustic phonon combinations occur. The second order features are labeled with their respective frequencies on the RT Raman spectrum. The most prominent second-order features occur in the high-frequency region and correspond to LO overtones and combinations involving LO modes. The broad peak at 1148 cm^{-1}, contains contributions of $2A_1$(LO) and $2E_1(LO)$ modes at the Γ point of the Brillouin zone, and possibly also of *2LO* scattering by mixed modes from the rather bands along the A-L-M-line. The vibrational peak at 1093 cm^{-1} can be attributed to *2LO* at the *H* and *K* points of the Brillouin zone. Finally a thin peak can be observed in the RT Raman spectrum at 1052 cm^{-1}, which we assign the mode to *TO+LO* combinations at the *A* and *H* points.

4 CONCLUSIONS

ZnO was obtained by means of CBD-AμW. The nanofilms were characterized structurally by means of X-ray diffraction, although could not determine the influence of the solution composition, considering to the zinc nitrate and urea. By EDS measurements obtained the chemical stoichiometry of the films. To the consider that each unit cell contains two Zn atoms for two O atoms is possible to establish that for a higher urea quantity the Zn incorporates interstitially and the chemical reaction is also slower. It carried out a detailed study of the Raman scattering of ZnO nanofilms for concentrations ranging from 1:1 up to 1.10. It has discussed the origin and assigned the main vibrational bands that are associated to the O and Zn sublattices.

5 REFERENCES

1. Nomura, K., Kamiya, T., Ohta, H., Ueda, K., Hirano, M., Hosono, H., "Carrier transport in transparent oxide semiconductor with intrinsic structural randomness probed using single-crystalline $InGaO_3(ZnO)_5$ films", Applied Physics Letters, Vol. 85, No. 11, pages 1993-1995, **2004.**

2. Hao, X. T., Tan, L.W., Ong, K. S., Zhu, F., "High-performance low-temperature transparent conducting aluminum-doped ZnO thin films and applications", Journal of Crystal Growth, Vol. 287, No. 1, pages 44-47, **2006**.

3. Ellmer, K., "Magnetron sputtering of transparent conductive zinc oxide: relation between the sputtering parameters and the electronic properties", Journal of Physics D: Applied Physics, Vol. 33, pages R17.-R32, **2000**.

4. Jagadish, C., Zinc Oxide Bulk, Thin Films and Nanostructures, First edition, Ed. Elsevier. England. **2006**.

5. Calleja, J. M., Cardona, M., "Resonant Raman scattering in ZnO", Physical Review B, Vol. 16, No. 8, pages 3753-3761, **1977**.

6. Cuscó, R., Alarcón-Lladó, E., Ibáñez, J., Artús, J., Jiménez, J., Wang, B., Callahan, M. J., "Temperature dependence of Raman scattering in ZnO", Physical Review B, Vol. 75, pages 165202-165202-11, **2007**.

7. Serrano, J., Romero, A. H., Manjón, F. J., Lauck, R., Cardona, M., Rubio, M. A., "Pressure dependence of the lattice dynamics of ZnO: An ab initio approach", Physical Review B, Vol. 69. pages 094306-1- 094306-14, **2004**.

8. Weinstein, B. A., "Pressure dependent optical phonon anharmonicity in GaP", Solid State Communications, Vol. 20, No. 10, pages 999-1003, **1976**.

9. Serrano, J., Manjón, F. J., Romero, A. H., Widulle, F., Lauck, R., Cardona, M., "Dispersive Phonon Linewidths: The E_2 Phonons of ZnO", Physical Review Letters, Vol. 90, No. 5, pages 055510-1- 055510-4, **2003**.